

The Cycling of Matter between Stars, the Interstellar Medium, and the Intergalactic Medium

A.G.G.M. TIELENS¹

¹*Leiden Observatory, Leiden University, the Netherlands*

ABSTRACT

The evolution of the interstellar medium is driven by a number of complex processes which are deeply interwoven, including mass accretion from nearby (dwarf) systems and the intergalactic medium, mass ejection into the halo and intergalactic medium, stellar mass injection into the interstellar medium, star formation, mechanical energy input by stellar winds & supernova explosions, and radiative energy input. These processes are mediated by dust and molecules in an only partially understood way. This complex feedback between stars and the medium they are formed in drives the evolution of galaxies and their observational characteristics.

SPICA is set to expand studies of the origin and evolution of the interstellar medium and its role in the evolution of galaxies to the era of vigorous star formation in the Universe at redshifts between 1 and 3. Yet, our understanding of what these observations tell us about what really happens at those epochs will depend very much on our understanding of the microscopic physical and chemical processes and their dependence on the local conditions. These are best studied in the local universe. In order to reap the full benefits of *SPICA*, a concerted program of key observations is required that study the physics and chemistry of the ISM locally and leverage this to probe the far Universe.

1. INTRODUCTION

The origin and evolution of galaxies are closely tied to the cyclic processes in which stars eject gas and dust into the interstellar medium (ISM), while at the same time gas and dust clouds in the ISM collapse gravitationally to form stars. The ISM is the birthplace of stars, but stars regulate the structure of the gas, and therefore influence the star formation rate. Winds from low mass stars — hence, the past star formation rate — control the total mass balance of interstellar gas and contribute substantially to the injection of dust, an important opacity source, and Polycyclic Aromatic Hydrocarbon molecules (PAHs), an important heating agent of interstellar gas. High mass stars (i.e., the present star formation rate) dominate the mechanical energy injection into the ISM, through stellar winds and supernova explosions, and thus the turbulent pressure which helps support clouds against galactic- and self-gravity. Through the formation of the hot coronal phase, massive stars regulate the thermal pressure as well. Massive stars also control the FUV photon energy budget and the cosmic ray flux, which are important heating, ionization, and dissociation sources of the interstellar gas. Massive stars are also the source of intermediate mass elements which play an important role in interstellar dust. Eventually, it is the dust opacity which allows molecule formation and survival. The enhanced cooling by molecules is crucial in the onset of gravitational instability of molecular clouds.

Clearly, therefore, there is a complex feedback between stars and the ISM. And it is this feedback that determines the structure, composition, chemical evolution, and observational characteristics of the interstellar medium in the Milky Way and in other galaxies all the way back to the first stars and galaxies that formed at redshifts > 5 . If we want to understand this interaction, we have to understand the fundamental physical processes that link interstellar gas to the mechanical and FUV photon energy inputs from stars.

SPICA provides a challenging opportunity to study the origin and evolution of the ISM of galaxies. As a powertool, *SPICA* provides access to key tracers of the interstellar medium including atomic and ionic fine-structure lines and molecular rotational lines — that can probe the physical conditions of the different components and phases of the ISM —, the emission features of PAH molecules — that play such an important role in the energy and ionization balance of interstellar gas as well as trace the interaction regions of massive stars with their environments —, and dust absorption and emission features as well as continuum — that trace the characteristics and origin of dust as well as acts as a proxy for gas. *SPICA* will be able to do so through the era of vigorous star formation in the history of the Universe (redshifts 1–3) when most stars were born and galaxy assembled. The challenge will be to validate and calibrate these tracers in the local Universe and to link them to the processes that drive the evolution of the ISM of galaxies.

In this review, I will focus on two key questions: *What are the sources of gas and dust ? & What processes play a role in the lifecycle between stars and the ISM ?*. I choose these two questions because the infrared can shine unique light on them. I will end with a short outline of some key issues that can be addressed well by *SPICA*.

TIELENS

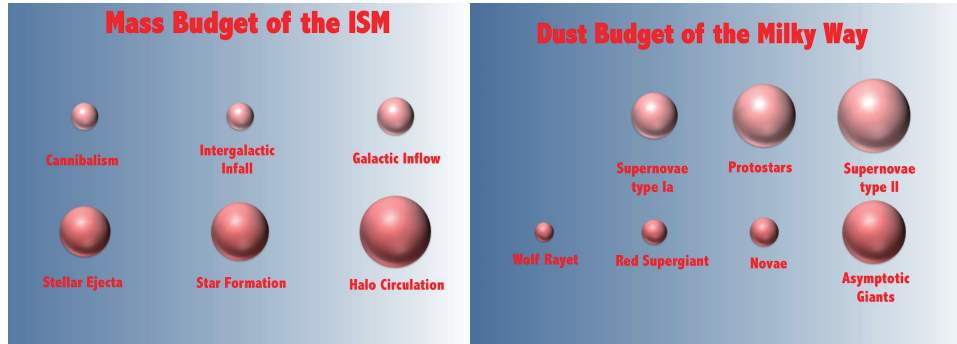


Figure 1. The gas (left) and dust (right) budgets of the Milky Way. The volume of the spheres indicates their relative importance. For details see Tielens (2005).

2. THE GAS AND DUST BUDGETS OF GALAXIES

Stars in the last stages of their evolution return much of their material to the ISM. For most stars, as these ejecta expand and cool, small dust grains nucleate and grow when the temperature drops to about 1500 – 1000 K, depending on the material and the chemical kinetics (Cherchneff 2000; Cherchneff & Dwek 2010). This dust, heated by stellar radiation, dominates the spectral energy distribution (SED) of the star and the mid- and far-infrared emission provides an excellent tracer of the mass. Fits to these SEDs provide then a handle on the dust injection rate, which can be translated into a gas mass loss rate adopting a dust-to-gas ratio and a velocity (Srinivasan et al. 2009). The gas can also be traced directly through molecular observations. Molecular excitation and uncertain abundances hamper analysis of these lines in terms of mass loss rates but the multitude of molecular lines can overcome this (Olofsson 2008). For some, mainly massive stars (OB & Wolf Rayet stars), mass loss is better traced by UV resonance lines, optical/IR wind emission lines, IR/radio thermal emission from the gas. For these sources, detailed empirical scaling laws have been derived linking the mass loss rate to the properties of the star (Vink et al. 2000).

The mass budget of the ISM is summarized in Figure 1 (Tielens 2005). Stars pollute the Milky Way with $\approx 2 M_{\odot}/\text{yr}$ of gas and associated dust and molecules. The gas return is dominated by the numerous low mass stars during their Asymptotic Giant Branch phase. Supernovae from massive stellar progenitors contribute only some 10% of the gas mass compared to low mass stars but a comparable amount of heavy elements, reflecting their factor 10 enrichment by nucleosynthesis. The timescale for stars to replenish the local interstellar gas mass is 5×10^9 years. This is very comparable to the star formation rate which converts the available gas mass into stars on a timescale of 3×10^9 years. The galactic fountain, setting up the circulation between the halo and the disk, involves more gas (e.g., $\approx 5 M_{\odot}/\text{yr}$). The Milky Way grows due to accretion of nearby dwarf galaxies — the Magellanic stream provides a prime example — but this cannibalism is only of minor importance for the overall mass balance. The G-star problem indicates that the Milky Way may have been accreting some $1 M_{\odot}/\text{yr}$ of metal-poor intergalactic gas over much of its history. Finally, the gas disk is very extended and this gas may slowly flow inwards replenishing gas lost to star formation in the inner disk. Unfortunately, existing evidence for radial motion may actually reflect non-axisymmetric distribution of gas in space or velocity and limits on inflow are very forgiving (≈ 5 km/s; Blitz, private communication). Table 1 adopts 1 km/s. It should be recognized that the magnitude of the various contributions to this mass budget are uncertain. Nevertheless, all of the processes involved are relatively rapid compared to the lifetime of the Milky Way and hence a quasisteady state has been established, balancing stellar mass injection and intergalactic mass accretion with star formation and mass loss. It should be recognized, though, that some of these processes are highly punctuated, driven by temporal interaction with nearby systems, and steady state may only apply averaged over long timespans.

Observations show that AGB stars are important contributors to the stardust budget of the Milky Way (Figure 1), returning some $6 \times 10^{-3} M_{\odot} \text{ yr}^{-1}$ in solid form. By comparison, red supergiants, the descendants of massive stars, return only a paltry $1.5 \times 10^{-4} M_{\odot} \text{ yr}^{-1}$ of dust. The contribution of SNe to the dust mass budget is unclear. If all the condensible material were turned into dust, type II SNe might contribute some $9 \times 10^{-3} M_{\odot} \text{ yr}^{-1}$. Observationally, dust is known to form typically between 300 and 1000 days after the SN explosion as revealed by a sudden drop in optical light, a concomittant increase in IR emission, and the development of a pronounced blue-red asymmetry in the emission line profiles of the ejecta (Wooden et al. 1993; Lucy et al. 1989). However, IR studies of core collapse SNe implied less than $5 \times 10^{-3} M_{\odot}$ of dust (somewhat dependent on the adopted grain material properties, very sensitive to the adopted clumpy distribution of the ejecta, and widely varying between SNe), corresponding to an efficiency of $\approx 10^{-3} - 10^{-1}$ (Wooden et al. 1993; Sugarman et al. 2006; Ercolano et al. 2007; Meikle et al. 2007). Young supernova remnants (SNR) provide another view of the dust formation efficiency of SNe and one that indicates much higher dust formation efficiencies. *Spitzer* studies of the young (≈ 330 yr) supernova remnant, Cas A, revealed a warm dust mass of $0.025 M_{\odot}$ in the volume processed by the reverse shock (Rho et al. 2008). A *Herschel* study adds to that $0.075 M_{\odot}$ of cold dust mass interior to the reverse shock (Barlow et al. 2010). The total dust mass ($\approx 0.1 M_{\odot}$) should be compared to the estimated total ejected mass of $2-4 M_{\odot}$, much of this in the form of oxygen ($\approx 2 M_{\odot}$) which will not condense (Willingale et al. 2002; Vink et al. 1996). In analogy to the

THE CYCLING OF MATTER IN THE UNIVERSE

Table 1. Inventory of the ISM

Component	Milky Way	LMC	SMC	unit
Total mass of dark halo	1×10^{12}	$\approx 1 - 3 \times 10^{10}$	$\approx 1.5 \times 10^9$	M_{\odot}
Stellar Mass	5×10^{10}	1.7×10^9	3.7×10^8	M_{\odot}
Gas				
ISM mass	7.5×10^9	5.2×10^8	4.2×10^8	M_{\odot}
Star formation rate	2	≈ 0.2	≈ 0.04	$M_{\odot} \text{ yr}^{-1}$
RSG & AGB Mass Loss	1	4×10^{-3}	1.4×10^{-3}	$M_{\odot} \text{ yr}^{-1}$
SNe	2×10^{-1}	$\approx 10^{-1}$	$\approx 3 \times 10^{-2}$	$M_{\odot} \text{ yr}^{-1}$
Z	1 ¹	0.5	0.1 – 0.2	Z_{\odot}
Dust				
ISM mass ²	6×10^7	$\approx 3.5 \times 10^6$	$\approx 3 \times 10^5$	M_{\odot}
RSG & AGB Mass Loss	6×10^{-3}	2×10^{-5}	$7 \approx 10^{-6}$	$M_{\odot} \text{ yr}^{-1}$
SNe production ³	9×10^{-3}	4×10^{-3} (?)	$1 - 40 \times 10^{-6}$	$M_{\odot} \text{ yr}^{-1}$
Dust destruction by SNe	$\approx 6 \times 10^{-3}$			$M_{\odot} \text{ yr}^{-1}$
Stellar astration of dust ⁴	2×10^{-2}	$\approx 3.5 \times 10^{-3}$	10^{-3} (?)	$M_{\odot} \text{ yr}^{-1}$

¹ The metallicity of the Milky Way shows a gradient of -0.06 dex per kpc in the primary elements. ² From COBE measurements of the IR emission for the Milky Way and $160 \mu\text{m}$ PACS/*Herschel* measurements for the LMC/SMC. ³ Assuming complete condensation of all dust forming elements. ⁴ Winds from young stellar objects may also inject newly formed dust into the ISM and this may amount to about 1/3 of this value. References: Tielens (2005); Srinivasan et al. (2009); Matsuura et al. (2009); Riedel et al. (2012); Matsuura et al. (2013); Meixner et al. (2013); Dwek et al. (1997)

well-studied type IIb SN 1993J, some $0.6 M_{\odot}$ of condensible elements (C, Mg, Si, S & Fe) were ejected during the SN explosion of Cas A (Thielemann et al. 1996), corresponding to a very high dust formation efficiency of ~ 0.2 . Likewise, *Herschel* observations of the extremely young SNR associated with SN 1987A — which has just entered the reverse shock phase as the ejecta slammed into the previous stellar wind remnant some 10 years after the explosion — reveal $\sim 0.5 M_{\odot}$ of cold dust (Matsuura et al. 2011); many orders of magnitude larger than estimated from observations during the dust condensation period of ~ 500 – 1000 days (10^{-4} – 10^{-3} ; Wooden et al. 1993). Given the bewildering zoo of SNe types and the uncertainties and conflicting observational results on dust formation in these environments, the contribution of SNe to the dust budget can presently only be guessed at but this anecdotal evidence suggests that it is high. Figure 1 assumes that all of the condensibles form dust and type II SNe are then slightly more important than AGB stars for the dust budget.

Figure 1 also includes a contribution of dust formed in the inner regions of protoplanetary disks and entrained and ejected by the protostellar wind. This estimate is also at the high end as it is based upon the assumption that 1/3 of the accreting mass is ejected as a wind (Shu & Shang 1997) and that all condensibles form dust. Other estimates of protostellar wind characteristics typically result in a ~ 3 times smaller wind mass loss rate (Hartmann 1995). It should also be kept in mind that, for the dust budget, protostellar winds are only a “pseudo” source of dust. The wind likely originates from the inner region where all preexisting dust has sublimated and recondensed. The net addition of dust may then actually be negative (carbon will not condense as dust in these environments). Certainly, in terms of the *stardust* budget of the ISM, astration by protostars presents a sink.

The main uncertainty in these mass injection rates has not yet been mentioned. Derived mass-loss rates depend directly on the distance and these are very uncertain for galactic objects. The SAGE/*Spitzer* and Heritage/*Herschel* programs have mapped the Small and Large Magellanic Clouds in all photometric bands between 3 and $500 \mu\text{m}$ and — because the distance is well known — the dust budget of these low metallicity dwarf galaxies has been well determined on a galaxy-wide scale (Srinivasan et al. 2009; Matsuura et al. 2009; Riedel et al. 2012). Results of these studies are summarized in Table 1. Perusal of this data reveals interesting similarities and differences between these galaxies. In particular, at the measured star formation rate, the existing gas reservoir will be consumed in some 3×10^9 yr for the Milky Way and the LMC, but that timescale is $\sim 10^{10}$ yr for the SMC. This gas reservoir will be replenished by stellar injection on timescales of $\approx 5 \times 10^9$ yr for the Milky Way and the LMC; so the gas content of these two galaxies is roughly in steady state. For the SMC, the relevant timescales are comparable (10^{10} yr) to the Hubble time and indeed the SMC is quite gas-rich compared to its stellar mass. Now, in contrast to the Milky Way, the gas budget of the SMC and LMC is dominated by SNe and not AGB stars. These dwarf galaxies are still undergoing strong bursts of star formation (Harris & Zaritsky 2009); e.g., the star formation rate of the LMC increased very rapidly some 5 Gyr ago and hence low mass stars when this burst started (or later)— formed at the start of this burst or later — have not yet had time to evolve onto the AGB. As a corollary, the measured dust injection rate by AGB stars cannot have provided the observed dust content of the SMC and LMC (Table 1). In contrast, SNe could have, if they are indeed efficiently producing dust (see above). Alternatively, for the Milky Way, we

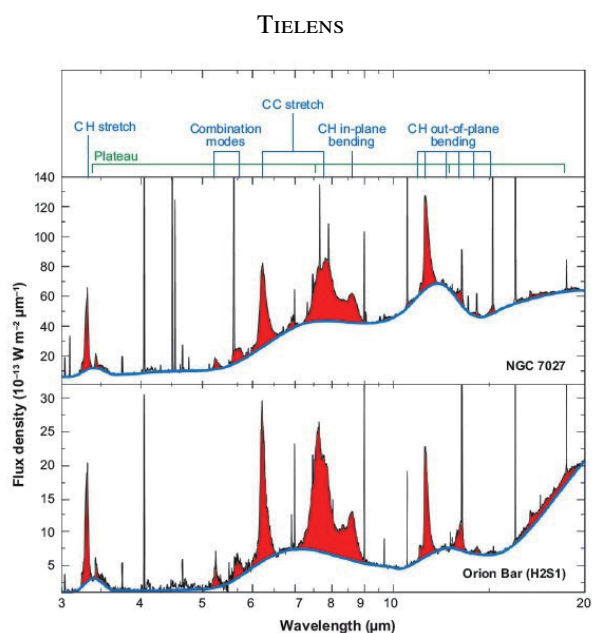


Figure 2. The mid-infrared spectra of the PhotoDissociation Region in the Orion Bar and in the Planetary Nebula, NGC 7027 are dominated by a rich set of infrared emission features. Assignments of these features with vibrational modes of PAH molecules are labeled at the top. These PAH features are perched on broad plateaus attributed to clusters of PAHs and on a mid-infrared continuum likely due to nanograins. Figure adapted from Peeters et al. (2002).

know that accretion of refractory elements such as Si, Mg, Fe on dust is very rapid in diffuse clouds (Savage & Sembach 1996; Tielens 1998) and hence much of the dust mass of the LMC and SMC may result from accretion on a few stardust grains injected by AGB stars.

3. THE ROLE OF PAHS IN THE ISM

The infrared spectra of almost all interstellar objects — including regions of massive star formation such as H II regions and reflection nebulae (Figure 2), carbon-rich stars in the last phases of their evolution such as post-Asymptotic-Giant-Branch stars and planetary nebulae, surfaces of dark clouds, the planet forming disks of young stellar objects, the general interstellar medium, galactic nuclei, and (ultra)luminous infrared galaxies — are dominated by strong, broad emission features at 3.3, 6.2, 7.7, 8.6, 11.2, and 12.7 μm (Figure 2; Peeters et al. 2002; Hony et al. 2001; Armus et al. 2007; Kaneda et al. 2013; Kim et al. 2012; Mori et al. 2012)). These strong emission features are accompanied by a plethora of weaker bands at 3.4, 5.2, 5.7, 6.0, 7.4, 12.0, 13.5, 14.2, 15.8, 16.4, 17.0, 17.4 μm and are perched on very broad plateaus and a continuum that is sharply rising towards longer wavelength (for a review, see Tielens (2008)). These features are ubiquitous in the interstellar medium on all scales from planet forming disks around young stellar objects to the scale of whole galaxies. It is clear that the carriers represent an important component of the ISM.

These spectral features are very characteristic in peak position for polycyclic aromatic hydrocarbon materials and they are generally ascribed to IR fluorescence of UV-pumped large Polycyclic Aromatic Hydrocarbon molecules (PAHs; Allamandola et al. 1989; Puget & Leger 1989; Tielens 2008). There are three pieces of evidence supporting the assignment of these features to large molecules (50–100 C-atoms) rather than “bulk” materials (e.g., 10–300 nm grains). (1) In order to emit in the mid-IR, the carrier(s) of the IR emission features must be much hotter than the 15 K that characterizes the far-IR emission due to 10–300 nm grains in radiative equilibrium with the interstellar radiation field. Hence, a fluorescence process is implied in which a single photon highly excites the molecule, which then relaxes through the emission of IR photons. Analysis of the energetics involved implies then molecular-sized carriers (50–100 C-atoms). (2) Several of the IR emission features (e.g., the 6.2 & 11.2 μm features) show a pronounced redshaded profile. Such a profile is characteristic for anharmonicity; again a distinct signature for emission by highly vibrationally excited molecules (Barker et al. 1987; Cook & Saykally 1998; Pech et al. 2002). (3) The feature to continuum ratio is very high, exceeding 20 in many sources. This is quite typical for molecular compounds; bulk (carbonaceous) materials, in contrast, invariably have intrinsic feature-to-continuum ratios that are much less.

Observations of the IR emission features and the spectroscopic, physical and chemical characteristics of interstellar PAHs have recently been reviewed elsewhere (Tielens 2008). Here, I highlight one aspect: the observed variations in the relative strength of the CH (3.3 and 11.2 μm features) to the CC modes (6.2 and 7.7 μm features). This illustrates well how observations of the IR emission features can be used to determine the physical conditions in regions of star formation. Such variations have been observed when comparing different sources as well as when comparing different positions within the same source (Galliano et al. 2008). The two spectra in Figure 2 illustrate these variations well. Extensive laboratory studies and quantum chemical calculations have demonstrated that, while peak positions can shift somewhat, the intrinsic

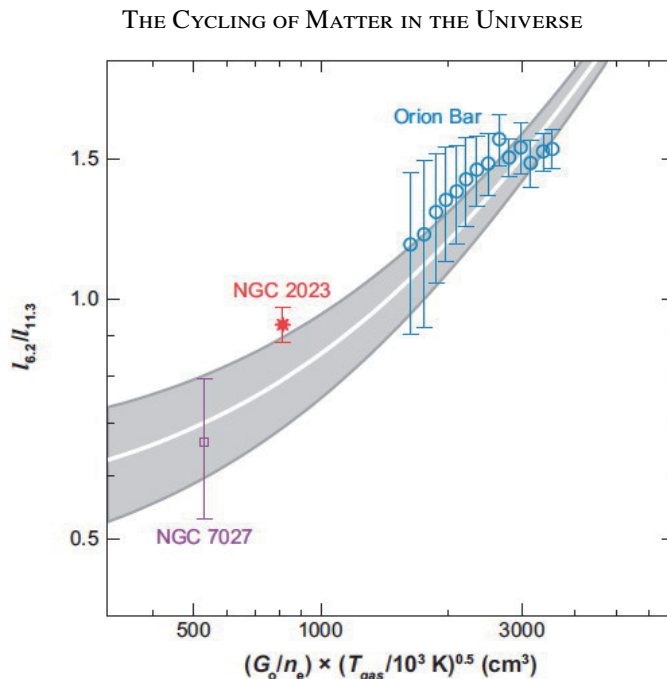


Figure 3. The observed ratio of the 6.2 to 11.2 μm bands — a measure of the degree of ionization of PAHs — is related to the ionization parameter, $(\gamma =)G_oT^{1/2}/n_e$ for a few well-studied PDRs, where the physical conditions — the strength of the UV radiation field, G_o , the electron density, n_e , and, the temperature, T — have been well determined from a multitude of atomic fine-structure lines and molecular rotational lines. The degree of ionization of PAHs increases to the right as either G_o increases or n_e , decreases. The temperature, T , enters through the velocity dependence of the Coulomb focusing factor. Figure taken from Galliano et al. (2008).

strength of modes involving CC stretching vibrations can increase manifold upon ionization while the CH stretching and to a lesser extent the out-of-plane bending vibrations decrease in strength (c.f., Allamandola et al. 1999; Langhoff 1996). Thus, the observed ratio of the 6.2 to the 11.2 μm bands is a direct measure of the ionized fraction of PAHs in the emission region with important ramifications for our understanding of the photo-electric effect (cf., Verstraete 2011; Tielens 2008) as well as for the ionization balance of interstellar gas. As a corollary, if we understand the physics and chemistry of interstellar PAHs and if we calibrate this ratio on local well-studied regions, observations of the PAH emission features can provide a handle on the physical conditions of the gas. This is illustrated in Figure 3 which gives the observed ratio of the CC-to-CH modes as a function of the ionization parameter, $\gamma = G_oT^{1/2}/n_e$ (Galliano et al. 2008). The ionization parameter is proportional to the ratio of the ionization rate over the recombination rate of a species and, hence, sets the charge.

4. THE DYNAMICS OF THE ISM

The mechanical energy input through expanding supernova ejecta and — to a lesser extent — by stellar winds has a profound influence on the structure of the ISM by generating turbulent motions of the H I and by sweeping up and shocking the surrounding interstellar gas to very high temperatures. Thus, while the total mechanical energy injected by massive stars into the ISM of the Milky Way is only a small fraction of the radiative energy budget ($L_{mech} \approx 2 \times 10^8 L_\odot$ versus $L_{rad} \approx 4 \times 10^{10} L_\odot$), the interstellar medium reacts to this mechanical energy by becoming very turbulent, the gas disk puffs up, and part of the volume becomes filled with hot gas. The latter may, even in the plane, become a dominant, separate phase of the ISM, the Hot Ionized (intercloud) Medium (HIM) in which the Warm Neutral/Ionized Medium and Cold Neutral Medium (e.g., diffuse clouds) are embedded. The importance of mechanical energy input for the structure of the ISM has been long recognized through UV absorption lines of highly ionized species e.g., O VI, N V, X-ray emission of hot gas, and large scale H I structures such as chimneys (Snowden et al. 1997; Heiles 1994; McCray & Snow 1979).

4.1. Interstellar Bubbles

Large scale, infrared surveys such as GLIMPSE and MIPS GAL with *Spitzer*, Hi-GAL with *Herschel*, and WISE have used dust emission as a tracer of the structure of the ISM of our galaxy and this has revealed that the ISM is a bubbly cauldron of activity where young, massive stars are strongly interacting with their environment (Figure 4; Churchwell et al. 2006). Assisted by volunteers from the general public, in excess of 5,000 “bubbles” have now been identified in IR images of the disk of our Milky Way galaxy (Simpson et al. 2012). These bubbles consist of bright 8 μm emission shells surrounding regions of bright 24 μm emission. These structures are thought to represent wind-blown-bubbles (Everett & Churchwell 2010) where the shock driven by the fast wind from a massive star ($v_w \sim 2000 \text{ km/s}$; $10^{-5} M_\odot/\text{yr}$) sweeps up the surrounding medium into a dense shell while the reverse shock heats the wind material to a high temperature ($3 \times 10^7 \text{ K}$; Weaver et al. (1977)). Gas near the inner boundary of this dense shell is then photo-ionized by the star and

TIELENS



Figure 4. A small portion of the GLIMPSE/MIPSGAL survey of the galactic plane reveals a myriad of bubbles (Churchwell et al. 2006). IRAC 8.0-micron light is green and MIPS 24-micron light is red.



Figure 5. *Left:* Multiwavelength image of the 30 Dor region in the LMC. Hot gas created by stellar winds and supernova explosions is traced by the X-ray emission (*blue*). Gas photo-ionized by the ~ 2400 massive OB stars in this super star cluster glows in the $H\alpha$ line (*Red*). The surrounding photodissociation region is traced by the IR emission from PAHs (*green*). This is an early stage of the formation of a superbubble. Eventually, such a superbubble will break out of the plane of the LMC. *Right:* A multi-wavelength, *Chandra*, *Hubble*, & *Spitzer* view of the M82 galaxy reveals a galactic wind — originating in the nucleus — venting out to distances of ~ 5 kpc into the halo. This wind, driven by the hot gas created by many SNe and traced by X-ray emission (*blue*), entrains gas and dust from the disk. The PAHs in these cloudlets are set aglow by UV star light (*red*). Shocked intercloud gas recombines and emits — among others — in $H\alpha$ (*orange*). The galactic disk is traced by the bluest visible light (*yellow-green*).

emits in, for example, $H\alpha$. Dust inside this ionized gas volume gets heated to a high temperature and emits in the mid-IR (e.g., $24\ \mu\text{m}$). PAHs in the surrounding photodissociation region are set aglow by FUV photons in the mid-IR emission features (Figure 4). Interpreting these structures as wind-blown-bubbles has some issues, though, as the expected, bright X-ray emission from the hot gas filling the bubbles has been notoriously difficult to observe and, indeed, for those sources where it has been observed, the X-ray emitting gas contains only a small fraction of the energy and mass of the stellar winds (Townsend et al. 2003). In addition, dust is not expected to survive under the harsh conditions of the hot bubble gas (Everett & Churchwell 2010). Furthermore, bubbles are also associated with stars that are suspected to have very weak winds; e.g., the wind mechanical energy is some 2% of the radiative energy for an O5 star but only 0.3 % for a B0 star. As an alternative interpretation, the observed structure of these bubbles may reflect the initial expansion of (radiatively) ionized gas into a medium with a pronounced density gradient followed by pressure release in a champagne flow into a surrounding low density environment when these bubbles burst (Ochsendorf et al., in preparation). The gas dynamics in combination with radiation pressure on the dust can then generate dust waves dominating the IR morphology of the region.

4.2. Galactic Winds & Halo-plane Interaction

Eventually, the massive stars blowing these bubbles will go supernova and a strong supernova shockwave will expand and sweep up the surrounding medium. A reverse shock will be driven into the ejecta heating the gas to $\approx 3 \times 10^7$ K (Figure 5). Massive stars are generally born in OB associations containing typically some 100 OB stars. The coalescence and rejuvenation of the hot gas by each successive SN will drive the formation and expansion of a superbubble. When this superbubble breaks out of the (cloud) disk, the energy will be vented into the halo — the galactic fountain — mixing material to great height and over large distances within the disk (c.f., Norman & Ikeuchi (1989)). Figure 5 shows a more extreme example of such a break-out associated with the moderate starburst in the nucleus of M82. Studies of IR emission from edge on galaxies have revealed that this levitation of dust is a common characteristic (Irwin et al. 2007; Thompson et al. 2004; Howk & Savage 1997; Burgdorf et al. 2007).

THE CYCLING OF MATTER IN THE UNIVERSE

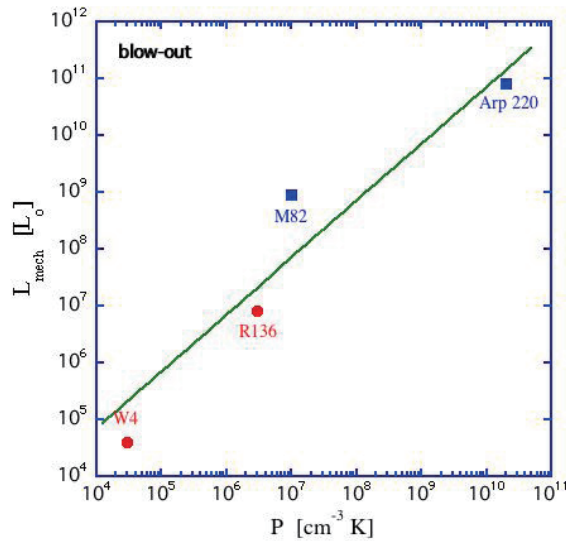


Figure 6. The mechanical luminosity derived from the observed supernova rate (assuming 10^{51} erg/SN) or the stellar wind is compared to the local interstellar medium pressure for a few well-chosen sources. The latter has been determined from observations of density/temperature sensitive atomic and/or molecular transitions. W4 has a well-developed superbubble, which has not (yet) broken out of the plane. R136 (and 30 Dor) are in the early stages of developing a superbubble. M82 has a well developed galactic wind originating in the numerous super star clusters in the nucleus. The ULIRG, Arp 220, has not (yet) developed a galactic wind. The line indicates Equation (4) for a coupling efficiency of $\xi = 0.1$.

The extreme star formation associated with the formation of super star clusters has thus a profound influence on the ecology of a galaxy and its subsequent evolution. To set the scale, a mini-starburst, such as R136 in the 30 Dor region has formed some 50 very massive stars and corresponds to a star formation rate, $SFR \sim 10^{-2} M_{\odot}/\text{yr}$. The whole 30 Dor region has been forming stars over a longer period (tens of millions of years) and is characterized by a $SFR \simeq 7 \times 10^{-2} M_{\odot}/\text{yr}$ (Doran et al. 2013). The nuclear starburst in M82 contains the equivalent of some 100 R136 and has a $SFR \sim 1 M_{\odot}/\text{yr}$. A ULIRG, such as Arp 220, has some 10,000 R136 and a $SFR \sim 10^2 M_{\odot}/\text{yr}$. Using a population synthesis model such as Starburst99 (Leitherer et al. 1999), these star formation rates can be translated into the radiative and mechanical energy input; viz.,

$$N_{Lyc} = 2 \times 10^{53} (SFR/M_{\odot}/\text{yr}) \quad \text{s}^{-1}, \quad (1)$$

$$\dot{M}_{\star} = 0.26 \times 10^{53} (SFR/M_{\odot}/\text{yr}) \quad M_{\odot}/\text{yr}, \quad (2)$$

$$L_{Mech} = 2 \times 10^8 (SFR/M_{\odot}/\text{yr}) \quad L_{\odot}. \quad (3)$$

Actually, of course, observations of the total infrared luminosity, the $H\alpha$ or $P\alpha$ line, are used to determine the star formation rate through equation (1) and similar ones. Equations (2) and (3) can then be used to determine the mass loss rate by massive stars and the mechanical luminosity. This does presume that the observed luminosity of a region reflects star formation activity rather than AGN activity. The importance of AGN activity may be judged from X-ray emission — but high column densities may hamper their detection —, from mid-IR emission lines from highly ionized species, or from the equivalent width of the PAH features (Genzel et al. 1998). Given the high obscuration that can be associated with extreme regions of star formation in galactic nuclei, much effort has been spent on developing other quantitative indicators for the star formation rate and validating them, using studies of local regions of star formation. These include the luminosity in the PAH features (Calzetti et al. 2007) and gas tracers of PDRs such as the CO lines (Tacconi et al. 2013).

We can also define a “blow-out” criteria; the minimum mechanical luminosity required for a superbubble to break out of the galactic disk,

$$L_{Mech} = 7 \times 10^7 \left(\frac{H}{\text{kpc}} \right)^2 \left(\frac{P}{10^7 \text{K cm}^{-3}} \right) \left(\frac{T}{10 \text{K}} \right) \left(\frac{0.1}{\xi} \right) \quad L_{\odot}, \quad (4)$$

with H , P , and T the scale height, pressure, and temperature of the gas in the disk and ξ the thermalization efficiency of the mechanical energy. The latter is estimated to be ~ 0.1 (Veilleux et al. 2005). Figure 6 collects data on a few well-chosen examples of star formation and superbubble formation. We note that regions of extreme star formation, such as ULIRGs, are characterized by high interstellar pressures, but nevertheless this data illustrates that breakout is happening/imminent

TIELENS

in all these environments. Regions of extreme star formation are therefore natural pollutants of galactic halo's and the intergalactic medium and the break out process will eventually limit extreme starbursts in ULIRG environments.

5. *SPICA'S VISION*

The evolution of the interstellar medium is driven by a number of complex processes which are deeply interwoven, including mass accretion, stellar mass injection, star formation, mechanical energy input by stellar winds & supernova explosions, and radiative energy input. The resulting ISM is highly structured where different phases interact and interchange dynamically on a rapid timescale. Moreover, the properties of the ISM are expected to vary systematically reflecting the local (stellar/ISM) conditions.

Dust and PAHs can be effective and quantitative tracers of many of these processes and infrared observations are key to this. Because of space limitations, I have not highlighted in this review IR observations of interstellar gas. The mid- and far-IR is home to key atomic and ionic fine-structure lines including [O I], [O III], [C II], [N II], [N III], [S I], [S III], [S IV], [Ar II], [Ar III], [Ne II], [Ne III], [Ne V], and [Si II] as well as the molecular rotational lines of H₂ and CO. Combined, these transitions are excellent tracers of the physical conditions of the emitting gas and hence can probe the physical conditions in warm interstellar regions. Large molecules and dust also play an active role in many of these processes but these links are only partially understood. Specifically, PAHs and dust couple gas thermodynamically to the non-ionizing stellar light through the photo-electric effect and dynamically through radiation pressure.

As the next generation infrared observatory, *SPICA* is well poised to address both aspects of ISM research using dust and PAH emission to trace the cyclical interrelationship of stars and the interstellar medium as well as quantify the detailed physics that drives this evolution in the near Universe and then use those relationships to understand the evolution of galaxies in the far Universe. Specifically, *SPICA* will be able to address many of the key questions in this field quantitatively and I am, particularly, looking forward to answers to the following:

- What are the *characteristics of interstellar dust* and how does that depend on metallicity, star formation activity, ISM conditions? How similar/different is dust formed in regions of extreme star formation from “local” dust and what does that tell us about the characteristics of dust in the earliest galaxies?
- What is the *role of PAHs and very small grains* in the energy & ionization balance of the ISM? And how does that influence the structure of the ISM and the star formation activity?
- What is the *role of mechanical energy* — SNR & turbulence — in the energy balance and phase structure of the ISM? How do supernova shocks process dust and PAHs and how does this couple back to the structure of the ISM and the star formation activity?
- What is the *role of the Halo and the IGM* in the mass, pressure, & energy budgets of the ISM?
- How can we best trace the *conditions for star formation* over the history of the Universe?

Studies of the interstellar medium, interstellar dust, and interstellar chemistry at Leiden Observatory are supported through advanced-ERC grant 246976 from the European Research Council, through a grant by the Dutch Science Agency, NWO, as part of the Dutch Astrochemistry Network, and through the Spinoza premie from the Dutch Science Agency, NWO.

REFERENCES

- Allamandola, L. J., Tielens, A. G. G. M., & Barker, J. R. 1989, ApJS, 71, 733
 Allamandola, L. J., Hudgins, D. M., & Sandford, S. A. 1999, ApJ, 511, L115
 Armus, L., et al. 2007, ApJ, 656, 148
 Barker, J. R., Allamandola, L. J., & Tielens, A. G. G. M. 1987, ApJ, 315, L61
 Barlow, M. J., Krause, O., Swinyard, B. M., et al. 2010, A&A, 518, L138
 Burgdorf, M., Ashby, M. L. N., & Williams, R. 2007, ApJ, 668, 918
 Calzetti, D., Kennicutt, R. C., Engelbracht, C. W., et al. 2007, ApJ, 666, 870
 Cherchneff, I., & Dwek, E. 2010, ApJ, 713, 1
 Cherchneff, I. 2000, in The Carbon Star Phenomenon, Proc. of IAU Symposium 177, p.331
 Churchwell, E., Povich, M.S., Allen, D., et al. 2006, ApJ, 649, 7
 Cook, D. J., & Saykally, R. J. 1998, ApJ, 493, 793
 Doran, E. I., Crowther, P. A., de Koter, A., et al. 2013, A&A, 558, A134
 Dwek, E., Arendt, R. G., Fixsen, D. J., et al. 1997, ApJ, 475, 565
 Ercolano, B., Barlow, M. J., & Sugerman, B. E. K. 2007, MNRAS, 375, 753
 Everett, J.E., & Churchwell, E. 2010, ApJ, 713, 592
 Galliano, F., Madden, S. C., Tielens, A. G. G. M., et al. 2008, ApJ, 679, 310
 Genzel, R., et al. 1998, ApJ, 498, 579

THE CYCLING OF MATTER IN THE UNIVERSE

- Harris, J. & Zaritsky, D. 2009, *ApJ*, 138, 1243
- Hartmann, L. 1995, *Revista Mexicana de Astronomia y Astrofisica Conference Series*, 1, 285
- Heiles, C. 1994, in *Physics of the Gaseous and Stellar Disks of the Galaxy*, ASP Conf. Ser., 66, p.249
- Hony, S., Van Kerckhoven, C., Peeters, E., et al. 2001, *A&A*, 370, 1030
- Howk, J. C., & Savage, B. D. 1997, *AJ*, 114, 2463
- Irwin, J. A., Kennedy, H., Parkin, T., & Madden, S. 2007, *A&A*, 474, 461
- Kaneda, H., Nakagawa, T., Ghosh, S. K., et al. 2013, *A&A*, 556, A92
- Kim, J. H., Im, M., Lee, H. M., et al. 2012, *ApJ*, 760, 120
- Langhoff, S. 1996, *J Phys Chem*, 100, 2819
- Leitherer, C., Schaerer, D., Goldader, J. D., et al. 1999, *ApJS*, 123, 3
- Lucy, L.B., Danziger, I.J., Gouiffes, C., & Bouchet, P. 1989, in *structure and dynamics of the interstellar medium*, eds. G. Tenorio-Tagle, M. Moles, J. Melnick, (Berlin: Springer Verlag), p164
- Matsuura, M., Barlow, M. J., Zijlstra, A. A., et al. 2009, *MNRAS*, 396, 918
- Matsuura, M., Dwek, E., Meixner, M., et al. 2011, *Science*, 333, 1258
- Matsuura, M., Woods, P. M., & Owen, P.J. 2013, *MNRAS*, 429, 5257
- McCray, R., & Snow, T. P. 1979, *ARA& A*, 17, 213
- Meikle, W. P. S., Mattila, S., Pastorello, A., et al. 2007, *ApJ*, 665, 608
- Meixner, M., Panuzzo, P., Roman-Duval, J., et al. 2013, *AJ*, 146, 62
- Mori, T. I., Sakon, I., Onaka, T., et al. 2012, *ApJ*, 744, 68
- Norman, C. A. & Ikeuchi, S. 1989, *ApJ*, 345, 372
- Olofsson, H. 2008, *Physica Scripta Volume T*, 133, 014028
- Pech, C., Joblin, C., & Boissel, P. 2002, *A&A*, 388, 639
- Peeters, E., Honny, S., Van Kerckhoven, C., et al. 2002, *A&A*, 390, 1089
- Puget, J. L., & Leger, A. 1989, *ARA&A*, 27, 161
- Riebel, D., Srinivasan, S., Sargent, B. & Meixner, M. 2012, *ApJ*, 753, 71
- Rho, J., Kozasa, T., Reach, W. T., et al. 2008, *ApJ*, 673, 271
- Savage, B. D., & Sembach, K. R. 1996, *ARA&A*, 34, 279
- Shu, F. H. & Shang, H. 1997, in *Herbig-Haro Flows and the Birth of Stars*, Proc. of IAU Symposium 182, 225
- Simpson, R. J., Povich, M. S., Kendrew, S., et al. 2012, *MNRAS*, 424, 2442
- Snowden, S. L., Egger, R., Freyberg, M. J., et al. 1997, *ApJ*, 485, 125
- Srinivasan, S., Meixner, M., Leitherer, C., et al. 2009, *AJ*, 137, 4810
- Sugerman, B. E. K., Ercolano, B., Barlow, M. J. et al. 2006, *Science*, 313, 196
- Tacconi, L. J., Neri, R., Genzel, R., et al. 2013, *ApJ*, 768, 74
- Thielemann F. K., Nomoto, K., Hashimoto, M.-A. 1996, *ApJ*, 460, 408
- Thompson, T. W. J., Howk, J. C., & Savage, B. D. 2004, *AJ*, 128, 662
- Tielens, A.G.G.M. 1998, *ApJ* 499, 267
- Tielens, A.G.G.M. 2005, *Physics and Chemistry of the Interstellar Medium*, (Cambridge: University of Cambridge Press)
- Tielens, A. G. G. M. 2008, *ARA&A*, 46, 289
- Townsley, L. K., Feigelson, E. D., Montmerle, T., et al. 2003, *ApJ*, 593, 874
- Verstraete, L. 2011, *EAS Publications Series*, 46, 415
- Veilleux, S., Cecil, G., & Bland-Hawthorn, J. 2005, *ARA&A*, 43, 769
- Vink, J., Kaastra, J. S., Bleeker, J. A. M. 1996, *A&A*, 307, L41
- Vink, J., de Koter, A., & Lamers, H. J. G. L. M. 2000, *A&A*, 362, 295
- Weaver, R., McCray, R., Castor, J. et al. 1977, *ApJ*, 218, 377
- Willingale, R., Bleeker, J. A. M., van der Heyden, K. J., et al. 2002, *A&A*, 381, 1039
- Wooden, D. H., Rank, D. M., Bregman, J. D. 1993, *ApJS*, 88, 477